Microscopic boundary layer model for a particle in entangled polymers: Steady-state particle diffusivity

W. Sung and Min Gyu Lee
Department of Physics, Pohang University of Science and Technology, Pohang, 790-784, Korea
(Received 22 February 1994)

A scheme for the microscopic theory of particle motion in a liquid of entangled polymers is presented. It is based on the model of a microscopic boundary layer, which appropriately combines a chain-dynamical description of microscopic response in particle-polymer interface with a hydrodynamical description of collective response in the polymer background beyond the interface. The scheme is applied to calculating the steady-state diffusivity of the particle.

PACS number(s): 61.41.+e, 66.30.Jt, 83.10.Nn, 83.20.Lr

I. INTRODUCTION

The dynamics of small particles dispersed in a liquid of entangled polymers is complicated in view of many-body dynamics of both the polymers and particles. Even in the simplest case of monodisperse spherical particles at very low concentration so that the interaction between the particles can be neglected, the particle-polymer interaction in the dynamical context remains a formidable problem to handle.

For large (spherical) particles suspended in a host liquid of viscosity η at an infinite dilution, a number of hydrodynamic results are well known. The diffusivity of a particle is given by the Stokes-Einstein relation [1]

$$D_{SE}=\frac{k_B T}{\zeta_S}\ , \tag{1}$$

where k_B is the Boltzmann constant and $\zeta_S=6\pi\eta R$ is the friction coefficient of the particle of radius R. The assumption behind this equation is that the particles are large enough to permit treatment of the background liquid as a continuum subject to the no-slip boundary condition. Therefore they do not incorporate microscopic details of the particle-polymer interface, which may be crucially important for the case of small particles approaching the mesh size of the polymers. To our knowledge, very little to date has been done toward generalizing the hydrodynamic results to the case of a small particle of arbitrary size. It is this case that we consider here.

An approach relatively simple but sensible enough to include the continuum limit as well as the interface structure which we introduce here is the model of the "microscopic boundary layer." This model was developed by Hynes, Kapral, and Weinberg [2] and Sung and Stell [3] for the problem of small-particle diffusion in the background of a small-molecule fluid. According to the model, the short-range dynamic interaction (collisional dynamics) between the particle and the background (fluid) within the interface is described in microscopic detail, while the long-range response of the background beyond the interface is treated collectively using hydrodynamic description. The key of the model is the generalized boundary condition obtained by matching these two descriptions at the outer boundary of the microscopic boundary layer. The model gave a successful description of short-range caging and long-range hydrodynamic feedback of the background, yielding an accurate estimate of the particle diffusivity for various ranges of particle size and fluid density [3]. When applied to a particle in a polymer, this model can be regarded as a polymer-dynamic analog of the Bethe-Peierls model [4], in the sense that the short-range interaction induced by the interface chains adsorbed on the particle and entangled with the background is treated microscopically, with the effect of all the distant chains upon the particle being treated only through a mean field (Fig. 1).

Our presentation of this work is as follows. In Sec. II, we construct the microscopic boundary layer specific to our polymer problem. On the basis of the elastically effective surface chains (ESC's) we determine the basic parameters of the boundary layers and construct the generalized boundary condition to couple the dynamics of the particle and ESC's to the background. While in this paper we are primarily concerned with development of the microscopic boundary layer model, in order to demonstrate its utility we apply these ideas to the problem of particle diffusion. Our development of the theory will be focused on the case of a spherical particle of arbitrary size and polymers of monodisperse molecular weight arbitrary but large enough to induce entanglements. Also it will be focused on the linear transport, the

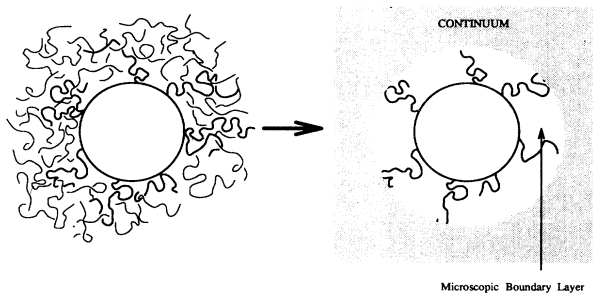

FIG. 1. The schematic picture of the microscopic boundary layer model.

steady-state diffusivity in particular, relevant to near-equilibrium situations where the fluxes and gradients are related linearly. The theory can be applied to the polymers not only in melts but also, under certain conditions, in solutions.

II. MICROSCOPIC BOUNDARY LAYER AND GENERALIZED HYDRODYNAMIC DESCRIPTION

The frictional force on the particle is dominantly due to the elastically effective surface chains, defined as the chains that remain grafted to the surface of the particle and entangled in the background chains at both ends, respectively, during the deformation and flow. We assume that such ESC's exist, either in chemical or in physical origin. The ESC's at equilibrium are constructed as shown in Fig. 2; the dangling chains and the loops not entangled in the background are not counted as such, and the number of ESC's is four in the case of Fig. 2.

The configuration of an ESC is, then, modeled as the particle-avoiding random walk that starts at a point $\vec{r}_0=R\hat{\vec{n}}_0$ on the surface and arrives at a position $\vec{r}$ after N_S steps without arriving at the surface on the way (Fig. 3). The problem is formulated in terms of the probability density $P_N(\vec{r})$ $(1\ll N\le N_s)$ with which the chain is found to be at $\vec{r}$ after N steps, subject to the boundary condition

$$P_N(\vec{r})=0 \quad \text{for } \vec{r} \text{ on the surface } (r=R) . \tag{2}$$

Under the assumption that the chain is ideal, $P_N(\vec{r})$ is governed by the diffusion equation

$$\frac{\partial}{\partial N}P_N(\vec{r})=\frac{b^2}{6}\nabla^2 P_N(\vec{r}) , \tag{3}$$

where b is the Kuhn step length. To solve for $P_N(\vec{r})$, we devise an image method, like that in electrostatics, where we superimpose two (Gaussian) solutions of Eq. (3):

$$P_N(\vec{r})=q_+\exp[-\alpha_+(\vec{r}-r_+\hat{\vec{n}}_0)^2] + q_-\exp[-\alpha_-(\vec{r}-r_-\hat{\vec{n}}_0)^2] . \tag{4}$$

Here q_+ and q_- are the weighting factors for the probabilities of random walks that start at r_+ and its image r_- (Fig. 3) which are positioned just outside and inside the surface in the immediate vicinity of $\vec{r}_0$ and along the normal direction $(\hat{\vec{n}}_0)$, and arrive at $\vec{r}$, respectively. Here $\alpha_+=3/2R_N^2$ and $R_N^2\equiv Nb^2$ is the mean-squared distance that the chains were to have in the absence of the particle and the background entanglements. To meet the boundary condition [Eq. (2)], one must have

$$\frac{r_+}{R}=\frac{R}{r_-} , \tag{5}$$

$$\alpha_+R^2=\alpha_-r_-^2 , \tag{6}$$

$$q_-=-q_+ . \tag{7}$$

From this, one obtains for an infinitesimally small but positive value of ϵ

$$r_\pm=R(1\pm\epsilon) , \quad \frac{\alpha_-}{\alpha_+}=1+2\epsilon , \tag{8}$$

and, finally, the probability density with which an ESC with N_s segments terminates at the position $\vec{r}$:

$$P_{N_s}(\vec{r})=\mathcal{N}(r^2-R^2)\exp[-R_s^{-2}(\vec{r}-\vec{r}_0)^2] . \tag{9}$$

Here $\mathcal{N}$ is the normalization constant and $R_s=\sqrt{2N_sb^2/3}$ is two times the radius of gyration of a free ideal chain with N_s segments, which serves as a characteristic length of the polymers in our problem. In Fig. 4, the probability $P_{N_s}(\vec{r})$ is plotted for various values of R/R_s. In the large-particle limit, $R/R_s\to\infty$, we recover the result of DiMarzio [5] for a flat surface,

$$P_{N_s}(\vec{r})\propto(\vec{r}\cdot\hat{\vec{n}}_0-R)\exp[-R_s^{-2}(\vec{r}-\vec{r}_0)^2] . \tag{10}$$

On the other hand, in the small-particle limit, $R/R_s\to 0$, we find an isotropic distribution,

$$P_{N_s}(\vec{r})\propto r^2\exp\left[-\left[\frac{r}{R_s}\right]^2\right] . \tag{11}$$

It is not surprising to find a deviation of the distribution from Gaussianity, which is nothing more than a characteristic of ESC defined as the particle-avoiding random walk.

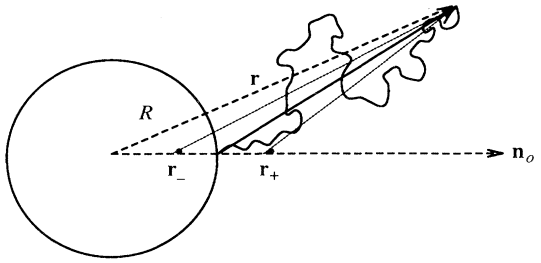

FIG. 3. An image method for calculating $P_N(\vec{r})$ of an ESC.

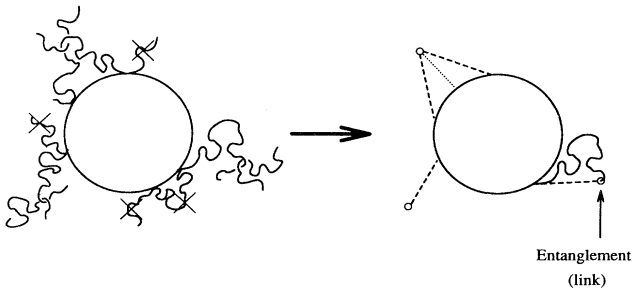

FIG. 2. Construction of the elastically effective surface chains (ESC's).

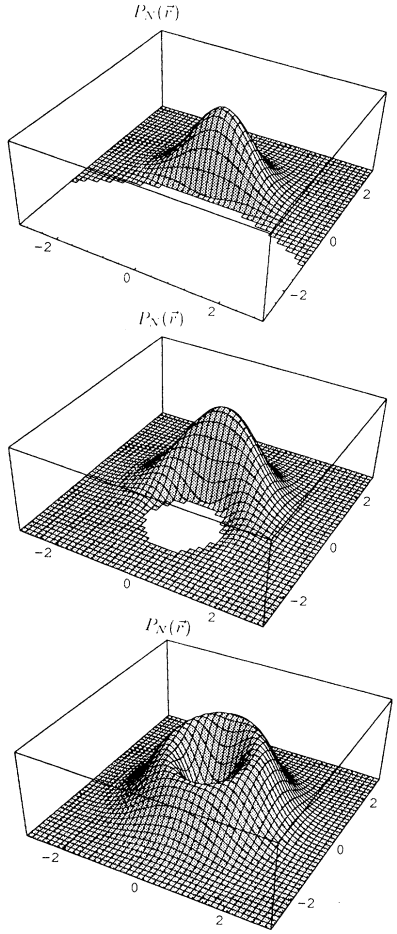

FIG. 4. The probability distribution $P_{N_s}(\vec{r})$ for an ESC. The starting point of ESC is $\vec{r}_0=(0.0)$ and all the lengths are in units of R_s. (a) $R/R_s=5$. (b) $R/R_s=1$. (c) $R/R_s=0.1$.

A. The boundary layer parameters, a and $\overleftrightarrow{\mathbf{K}}$ and α

The free energy $\mathcal{A}$ of an ESC with the ends at $\vec{r}_0=R\hat{\vec{n}}_0$ and $\vec{r}$ is

$$\mathcal{A}(\vec{r})=-k_BT\ln P_{N_s}(\vec{r})+\text{const}$$
$$=k_BT\{R_s^{-2}(\vec{r}-R\hat{\vec{n}}_0)^2-\ln(r^2-R^2)\}+\text{const}\ , \tag{12}$$

and the associated force on the chain end at $\vec{r}$ is

$$\vec{f}_S=-\vec{\nabla}\mathcal{A}(\vec{r})=-k_BT\vec{\nabla}\ln P_{N_s}(\vec{r})\ . \tag{13}$$

We define the thickness a of the microscopic boundary layer to be the radial distance from $\vec{r}_0$ to the position $\vec{r}^*$ of $\vec{r}$ where $\mathcal{A}$ is minimized [i.e., where $P_{N_s}(\vec{r})$ is maximized]. This definition, $a\equiv r^*-R$, enables us to determine it as a root of the cubic equation

$$\left[\frac{a}{R_s}\right]^2(a+2R)-(a+R)=0\ . \tag{14}$$

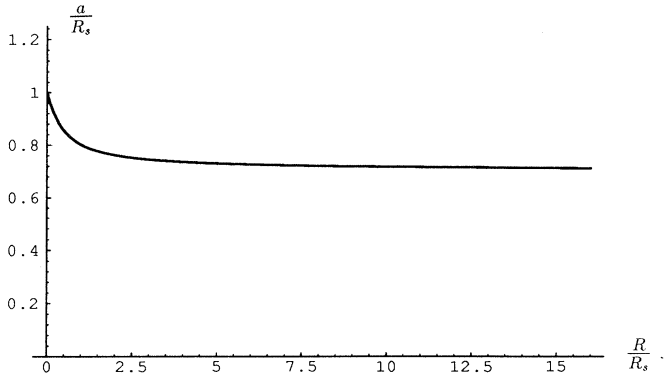

FIG. 5. The boundary layer thickness a (in units of R_s) vs R/R_s.

For infinitely large and small particle limits, it is obtained, respectively, as

$$a_\infty=\sqrt{1/2}R_s\ , \tag{15}$$

$$a_0=R_s\ . \tag{16}$$

The boundary layer thickness a defined in this way is plotted in Fig. 5 as a function of the particle's radius R. It is interesting to observe that, with N_s (or R_s) fixed, the a does not vary appreciably with R, especially for the values of R larger than R_s, say, by about ten times. With the end at the position $\vec{r}^*$, the chain has the minimum free energy and suffers no force. Associated with a small deviation $\delta\vec{x}$ of the end point away from $\vec{r}^*$ is the chain force $\vec{f}_s$ on an ESC given as

$$\vec{f}_S=-\overleftrightarrow{\mathbf{K}}\cdot\delta\vec{x}\ . \tag{17}$$

The entropic spring constant tensor $\overleftrightarrow{\mathbf{K}}$ is given as

$$\overleftrightarrow{\mathbf{K}}\equiv\vec{\nabla}\vec{\nabla}\mathcal{A}(\vec{r})|_{\vec{r}=\vec{r}^*=(R+a)\hat{\vec{n}}_0}$$
$$=2\frac{k_BT}{R_s^2}\left[\frac{R}{a+R}\overleftrightarrow{\mathbf{1}}+2\left[\frac{a}{R_s}\right]^2\hat{\vec{n}}_0\hat{\vec{n}}_0\right]$$
$$\equiv K_0\overleftrightarrow{\mathbf{1}}+K_1\hat{\vec{n}}_0\hat{\vec{n}}_0\ , \tag{18}$$

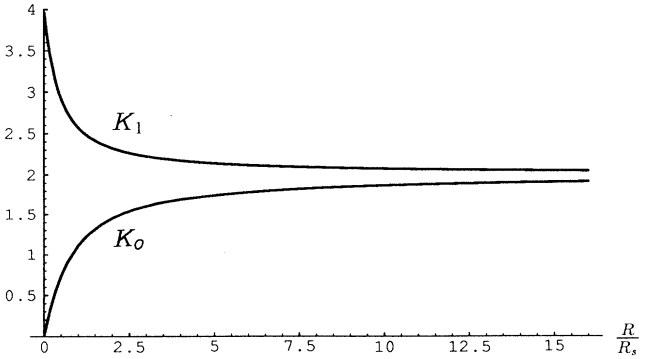

FIG. 6. The spring constants K_0 and K_1 (in units of k_BT/R_s^2) vs R/R_s.

where

$$K_0=\frac{2k_BT}{R_s^2}\frac{R}{a+R}\ , \tag{19}$$

$$K_1=\frac{4k_BT}{R_s^2}\left[\frac{a}{R_s}\right]^2 \tag{20}$$

are the isotropic and the anisotropic spring constants. As shown in Fig. 6, the constant K_0 approaches zero for small particles but approaches K_1 for large particles.

Another important parameter in our theory is the number of elastically effective surface chains within the boundary layer. We suppose that the α, the number of ESC's per unit area counted at the outer boundary surface (at $r=r^*=R+a$), hereafter termed S_0, is uniform over the surface.

The parameter α depends upon the surface chemistry as well as the polymer, but it can be presumed to be an independent variable. The parameters N_s and a are interdependent functions of R and α as well as the polymers in bulk.

B. The generalized boundary condition and hydrodynamics

Now consider the dynamic situation, in which the particle is moving while ESC's remain attached on the surface and entangled with the background chains (Fig. 7). In the steady state, Eq. (17) is replaced by the expression for the frictional force,

$$\vec{f}_s=-\overleftrightarrow{\mathbf{K}}\cdot\tau_D[\vec{u}-\vec{V}-\vec{\Omega}\times R\hat{\vec{n}}_0]\ , \tag{21}$$

where $\vec{u}$ is the average velocity of the entanglement [at the point $\vec{r}=(R+a)\hat{\vec{n}}_0$] with which the ESC is engaged and $\vec{V}$, $\vec{\Omega}$ are the average translational velocity and the rotational velocity of the particle. Within the linear response regime near equilibrium we consider here, the rotation is not coupled to the translation and will be neglected for our problem of translational diffusion. The time τ_D is the time during which a background chain remains engaged with an ESC (Fig. 7). We assume that it is the reputation time or disengagement time of an entangled chain in the bulk given by the theories of de Gennes [6] and Doi and Edwards [7] and is given by

$$\tau_D=\frac{\zeta_1N^3b^4}{12k_BTR_e^2}\propto N^3 \tag{22}$$

or experimentally $\tau_D\propto N^{3.4}$. Here, N is the number of segments in the chain in the bulk, ζ_1 is the (Rouse) friction coefficient of a segment, and R_e is the chain length between the adjacent enlargements. The strong dependence of τ_D on N implies that, for long polymers, the frictional force on a particle is dominated by the effect of entanglements and is indeed given by Eq. (21).

Supposing that the α, the surface number density of elastically effective surface chains, takes the steady state value, the chain statistical force per unit area at an arbitrary point positioned at $\vec{r}=(R+a)\hat{\vec{n}}$ on the outer surface S_0 is given by

$$\vec{F}=-\alpha\overleftrightarrow{\mathbf{K}}\cdot\tau_D(\vec{u}-\vec{V})\ . \tag{23}$$

Here $\overleftrightarrow{\mathbf{K}}$, $\vec{u}$ take the values evaluated at the point. Now, in the viewpoint of the background polymers beyond the boundary layer, the force is to be regarded as the hydrodynamic stress within our avowed theoretical scheme:

$$\vec{F}=\hat{\vec{n}}\cdot\overleftrightarrow{\sigma}\ . \tag{24}$$

In the above, $\overleftrightarrow{\sigma}$ is the hydrodynamic stress tensor at the point with a Cartesian component

$$\sigma_{ij}=p\delta_{ij}-\eta(\vec{\nabla}_iu_j+\vec{\nabla}_ju_i)\quad(i,j=1,2,3)\ . \tag{25}$$

Here p is the static pressure, η is the steady-state and zero-shear-rate viscosity of the background polymer fluid (melt or solution), and $\vec{u}$ is the fluid velocity. With this fluid velocity identified as the average velocity of the entanglement at the point $\vec{r}=(R+a)\hat{\vec{n}}$ at the outer boundary, matching Eq. (23) with Eq. (24) yields the generalized boundary condition on S_0,

$$-\alpha\overleftrightarrow{\mathbf{K}}\cdot\tau_D(\vec{u}-\vec{V})=\hat{\vec{n}}\cdot\overleftrightarrow{\sigma}\ . \tag{26}$$

The condition provides a machinery to describe the coupled dynamics of the particle and the background polymers, incorporating the microscopic interface chain effect hydrodynamically in a self-consistent way.

The next task is to solve, for the bulk region $r>R+a$ but subject to the boundary condition [Eq. (26)], the hydrodynamic equation

$$\vec{\nabla}\cdot\overleftrightarrow{\sigma}=0\ , \tag{27}$$

supplemented by the condition of incompressible flow

$$\vec{\nabla}\cdot\vec{u}=0\ . \tag{28}$$

Equations (27) and (28) are natural consequences of the conditions of linear and steady-state flow, to which we confine ourselves here.

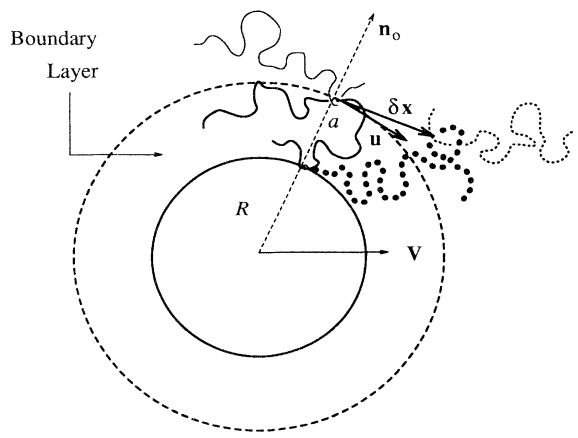

FIG. 7. The configurational change of an ESC during τ_D coupled both with a reptating chain and the particle in motion.

III. STEADY-STATE DIFFUSIVITY OF A PARTICLE IN ENTANGLED POLYMERS

In this section, we apply the scheme of generalized hydrodynamics developed in the foregoing section to the problem of diffusivity of a particle of an arbitrary size in a liquid (either a melt or a solution) of entangled polymers. The diffusivity of the particle is related to the friction coefficient via the Einstein relation

$$D=\frac{k_BT}{\zeta} . \tag{29}$$

The friction coefficient ζ is determined from the drag on the particle, which is the stress integrated over the outer boundary (S_0); using Eqs. (23) and (24), the drag is given as

$$\alpha\tau_D \oint_{S_0} (\vec{u}-\vec{V})\cdot\vec{\vec{K}}\, dS = -\oint_{S_0} \vec{\sigma}\cdot\hat{n}\, dS = -\zeta\vec{V} , \tag{30}$$

if the particle is set into motion with a velocity $\vec{V}$ in the polymer fluid initially at rest.

The procedure of solving the hydrodynamic equations for the friction is nothing more than the usual one of Stokes flow [8], except for our generalized boundary condition. We only quote our result for the fluid velocity field for $r>R+a$ subject to the boundary condition [Eq. (26)]:

$$\vec{u}(\vec{r})=\frac{1}{C}\left[Ar^{-1}-\frac{1}{3}Br^{-3}\right]\vec{V} + \frac{1}{C}\left[Ar^{-3}+Br^{-5}\right](\vec{V}\cdot\vec{r})\vec{r} , \tag{31}$$

where

$$A=3(R+a)\gamma\left\{6+\gamma+\frac{K_1}{K_0}(2+\gamma)\right\} , \tag{32}$$

$$B=-3(R+a)^3\left\{6+\gamma+\frac{K_1}{K_0}\gamma\right\} , \tag{33}$$

$$C=2\left\{18+15\gamma+2\gamma^2+\frac{K_1}{K_0}(6\gamma+2\gamma^2)\right\} . \tag{34}$$

Here $\gamma=K_0\alpha\tau_D(R+a)/\eta$. Using Eq. (19) this parameter can also be written as

$$\gamma=\frac{2k_BT\tau_D}{R_s^2\eta}\alpha R . \tag{35}$$

As the result of integrating the hydrodynamic response for ζ in Eq. (30), we find

$$\zeta=\frac{\zeta_h\zeta_e}{\zeta_h+\zeta_e} , \tag{36}$$

where

$$\zeta_h=6\pi\eta(R+a)\left[1-\frac{K_1}{K_0(6+\gamma)+K_1(3+\gamma)}\right] , \tag{37}$$

$$\zeta_e=4\pi(R+a)^2\alpha K_1\tau_D\left[\frac{K_0}{K_1}+\frac{2+\gamma}{6+\gamma}\right] . \tag{38}$$

For the γ defined in Eq. (35), we note that $\eta=G\tau_D$ where $G=cb^2k_BT/R_e^2$ is the plateau modulus of the polymers, c is the segment number density (concentration), and R_e is the root-mean-squared distance between entanglements. Then, we can rewrite

$$\gamma=\frac{R}{R_c} , \tag{39}$$

where

$$R_c=\frac{1}{2}\left[\frac{R_s}{R_e}\right]^2\frac{cb^2}{\alpha} \tag{40}$$

is a crossover length which has, if any, weak particle-size dependence.

Let us confine ourselves to the condition $R\gg a$, as is usual with colloidal particles larger than 0.1 μm, with boundary layer size a less than 100 Å. In these cases, our hydrodynamic treatment of the background polymer is expected to be at its best. Then, from Eqs. (19) and (20), we have $K_0/K_1\simeq 1$ and

$$\frac{\zeta_e}{\zeta_h}\simeq\frac{2\gamma}{3}\left[\frac{1+(2+\gamma)/(6+\gamma)}{1-1/(9+2\gamma)}\right] , \tag{41}$$

which is almost linearly increasing with γ.

Therefore, for particles small so that $\gamma\ll 1$ (but still $R\gg a$), we have $\zeta_e\ll\zeta_h$ and

$$\zeta\simeq\zeta_e\simeq 4\pi R^2\alpha\tau_D\left[K_0+\frac{1}{3}K_1\right]=\frac{16\pi k_BT}{3a^2}\tau_D\alpha R^2 , \tag{42}$$

where we used Eqs. (19) and (20) along with Eq. (15). Equation (42) accounts for the friction caused entirely by the elastically effective surface chains which remains entangled during the reputation time τ_D. Reasonably enough, it is proportional to τ_D, α as well as R^2. All the distant chains beyond the boundary layer do not affect the friction at all for this case of small particles. In connection with this short-range nature of the background polymer effect, it is important to note that the hydrodynamic disturbance as manifest in $\vec{u}(\vec{r})$ [Eq. (31)] tends to be also short ranged [$\vec{u}(\vec{r})\sim r^{-3}$] for small particles ($\gamma\ll 1$), compared with that of the Stokes flow, for which $\vec{u}\sim r^{-2}$.

On the other hand, for large particles ($\gamma\gg 1$), we find $\zeta_e\gg\zeta_h$ and

$$\zeta\simeq\zeta_h\rightarrow\zeta_S=6\pi\eta R , \tag{43}$$

the Stokes friction we expect to recover in this limit. This result is entirely insensitive to the microscopic details of the interface, as expected, provided that the chain anchorage α exceeds a certain critical value [13].

To better appreciate the dynamics involved for the particles of intermediate size, we consider the diffusivity, which is given via the Einstein relation using the friction coefficient [Eq. (36)] as

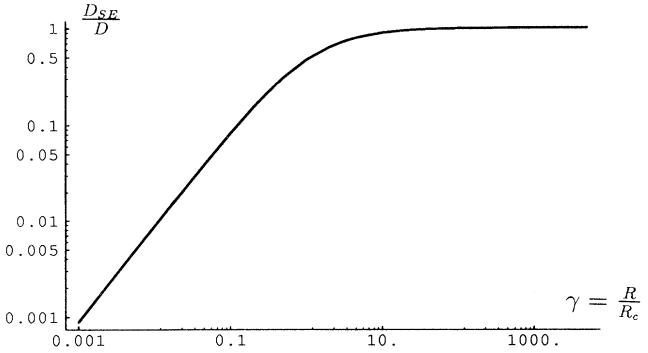

FIG. 8. D_{SE}/D as a function of $\gamma = R/R_c$.

$$D = \frac{k_B T}{\zeta} = D_e + D_h \ , \tag{44}$$

where

$$D_e = \frac{k_B T}{\zeta_e} \quad \text{and} \quad D_h = \frac{k_B T}{\zeta_h} \ . \tag{45}$$

The remarkable additivity of two diffusion constants, typical of the mode-coupling theory [9] and similar to the case of the particle in small-molecule fluids [2,3], implies that two dynamical processes are involved. The first one is the disengagement (constraint release) of elastically effective surface chains from the entanglements during the time τ_D. The other one is the relatively slow process of the long-range hydrodynamic feedback of the distant chains. Since these dynamic modes operate on distinct time scales, the diffusivity appears to be the sum of their contributions, as will be more evident in our forthcoming paper on the velocity autocorrelation function of the particle. For contrast, it is worthwhile to note that the self-diffusivity of a polymer is also given as the sum of the short-range constraint release and the tube release contributions [10].

For large particles ($\gamma \gg 1$), the diffusivity [Eq. (44)] approaches the hydrodynamic result of Stokes-Einstein [D_{SE} in Eq. (1)],

$$D \simeq D_h \rightarrow D_{SE} = \frac{k_B T}{6\pi\eta R} \propto R^{-1} \ . \tag{46}$$

For small particles ($\gamma \ll 1$), however, the disengagement of ESC dominates the hydrodynamic feedback, yielding

$$D \simeq D_e \rightarrow \frac{3a^2}{16\pi} \tau_D^{-1} \alpha^{-1} R^{-2} \propto R^{-2} \ . \tag{47}$$

For arbitrary size, the two dynamical processes behind D_h and D_e compete as shown in Fig. 8, which plots D_{SE}/D as a function of γ.

Although not conclusive yet, it is encouraging to find that these two particle-size dependences were observed experimentally [11], and it would be interesting to verify also other theoretical aspects predicted here. The crossover in the different size dependence (associated with the two dynamical processes mentioned above) occurs around $\gamma \simeq 1$ corresponding to the particle radius $R \simeq R_c$. [Eq. (40)].

IV. CONCLUSION

We modeled the microscopic boundary layer to describe the dynamics of a spherical particle in a liquid of entangled polymers. To this end, we introduced the elastically effective surface chain as the particle-avoiding random walk and determined the boundary layer size. By matching the dynamics of the ESC's to the hydrodynamics of the distant chains, we established the generalized boundary condition, subject to which the background response is to be calculated in a self-consistent manner.

To demonstrate its utility, we applied the model to the problem of steady-state diffusivity of the particle of arbitrary size. The model recovers the Stokes-Einstein result in the large-particle limit and gives a very reasonable result for small particles. For the general case, we found an analytical expression which encompasses the short-range (caging) dynamics of the particle with the anchored chain entangled with the background as well as the long-range dynamics of hydrodynamic feedback, best represented in small- and large-particle limits, respectively.

Further application of the model is at hand. In forthcoming papers, we will investigate the particle dynamics on various time scales as probed by the velocity autocorrelation function and the viscoelastic effect of the particle suspensions in polymers. Also of interest are the slippage problems [12,13] of entangled polymer liquids flowing on a wall, on which our model has some bearing when the presence of ESC's is unavoidable. From various studies of these aspects, it appears that the microscopic boundary layer model provides a useful and powerful analytical means of implementing the dynamical interaction between polymers and the particle or the surface.

ACKNOWLEDGMENTS

This work was supported in part by BRSC and CAMP of POSTECH, each funded by Ministry of Education of Korea and KOSEF. We also acknowledge the support of RIST and the Center for Thermal and Statistical Physics at Korea University funded by KOSEF Grant No. 93-08-00-05).

[1] A. Einstein, *Investigations on the Theory of the Brownian Movement* (Dover, New York, 1956).
[2] J. T. Hynes, R. Kapral, and M. Weinberg, J. Chem. Phys. **70**, 1456 (1979).
[3] W. Sung and G. Stell, J. Chem. Phys. **80**, 3350 (1984).
[4] H. A. Bethe, Proc. R. Soc. London, Ser. A **150**, 552 (1935).
[5] E. A. DiMarzio, J. Chem. Phys. **42**, 2101 (1965).
[6] P. G. de Gennes, J. Chem. Phys. **55**, 572 (1971).

[7] M. Doi and S. F. Edwards, *The Theory of Polymer Dynamics* (Oxford University Press, Oxford, 1986).
[8] L. D. Landau and E. M. Lifshitz, *Fluid Mechanics* (Pergamon, London, 1984).
[9] D. Bedeaux and P. Marzur, Physica (Utrecht) **76**, 235 (1974).
[10] W. W. Graessly, Adv. Polym. Sci. **47**, 67 (1982).
[11] H. Sillescu (private communication).
[12] P. G. de Gennes, C. R. Seances Acad. Sci. Ser. B **288**, 219 (1979); F. Brochard and P. G. de Gennes, Langmuir **8**, 3033 (1992); K. B. Migler, H. Hervet, and L. Leger, Phys. Rev. Lett. **70**, 287 (1993); A. Ajdari, F. Brochard, P. G. de Gennes, L. Leibler, J. Viovy, and M. Rubinstein, Physica A **204**, 17 (1994).
[13] W. Sung, Phys. Rev. E **51**, 5862 (1995).

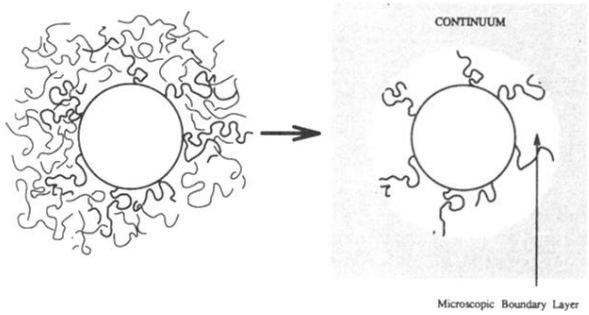

FIG. 1. The schematic picture of the microscopic boundary layer model.